

Silica Gel-Glasses Doped with Cr-Containing Nanoparticles

G. E. Malashkevich^a, G. I. Semkova^a, A. V. Semchenko^b,
P. P. Pershukevich^a, and I. V. Prusova^a

^a Stepanov Institute of Physics, National Academy of Sciences of Belarus, Minsk, 220072 Belarus

e-mail: g.malashkevich@ifanbel.bas-net.by

^b Gomel State University, Gomel, 246699 Belarus

Received October 21, 2008

Transparent silica glasses doped with heat-resistant luminescent nanoparticles with Cr³⁺ ions in the “strong” octahedral crystal field at the sol stage have been synthesized through the direct sol–gel–glass transition. Their electron microscopy and luminescence spectral studies have been performed. It has been found that the nanoparticles incorporated in these glasses are subject to the isotropic compression by the matrix and to slight dissolution (due to the absence of the melt stage) when the optical Crⁿ⁺ centers ($n = 3–6$) are formed.

PACS numbers: 42.70.Ce, 42.70.Hj, 78.55.Qr, 78.67.Br

DOI: 10.1134/S0021364008230082

The development of new methods for producing glassy materials with efficient luminescent nanostructures is dictated by the necessity of the continuous improvement of the active components for quantum electronics and rapidly developing nanophotonics. Usually, nanostructures in glasses are prepared by isothermal annealing. However, attempts to retain the nanoparticles of activator compounds in glasses have failed because these nanoparticles dissolve in the melt [1]. Owing to the development of the sol–gel technology, the glasses can be produced through bypassing the melt stage. This makes it possible to form their nanostructure by introducing such nanoparticles at the sol stage. However, these experiments have not yet been described in published data. Probably, this is mainly because it is difficult to produce nanoparticles that can be suspended in the sol at least until the gel starts to form and have a melting point appreciably higher than the pore healing temperature in the gel–glass matrix. It has been shown earlier [2] that efficiently luminescent heat-resistant nanoparticles with the agglomerate size <500 nm can be obtained by doping an ultradispersed diamond with Cr and some buffer elements. After heat treatment in air at $T \geq 1000^\circ\text{C}$, these particles are characterized by the Cr³⁺ ion luminescence in a narrow spin-forbidden band ${}^2E \rightarrow {}^4A_2$ split into two R lines. On the contrary, silica gel-glasses that are doped with the trivalent Cr salts and are sintered in air have broad luminescence bands with maxima at $\lambda_{\text{max}} \sim 660$ nm [3, 4] and 1.5 μm [5]. The former band is most likely attributed to the Cr⁵⁺ ions [6], while the latter band, by the Cr⁴⁺ ions [7]. Therefore, the possibility of the conservation of the structure of such Cr-containing nanoparticles in the sol–gel–glass transition can be analyzed by spectral-luminescence and electron microscopy meth-

ods. These studies are also interesting in application to the preparation of glassy materials with the spectral-luminescence characteristics similar to those of ruby.

The gel-glass synthesis included the hydrolysis of tetraethylorthosilicate Si(OC₂H₅)₄ in an aqueous acid solution until sol is formed, the addition of aerosil and Cr-containing nanoparticles to the sol prepared, the ammonia neutralization of the sol–colloid system, gel formation, and the drying and vitrification of xerogels in air at $T \approx 1240^\circ\text{C}$ for 1 h. The Cr-containing nanoparticles were obtained by the heat treatment of an ultradispersed raw diamond doped with Cr and buffer elements in air [2] and were then additionally milled to eliminate the coarsest agglomerates.

The glass microstructure was studied on a LEO-1420REM scanning electron microscope. The light attenuation spectra (LASs) were recorded on a Cary 500 spectrophotometer. The luminescence spectra (LSs) and luminescence excitation spectra (LESs) were recorded by the “reflection” method on an SDL-2 spectrofluorimeter. The LSs and LESs were corrected with regard to the spectral sensitivity of the recording system and the spectral density distribution of exciting radiation, respectively, and were expressed as the dependence of the number of photons per unit wavelength range $dN/d\lambda$ on the wavelength λ . All the measurements were carried out at $T = 298$ K.

Figure 1 presents the microphotographs of (a) Cr-containing nanoparticles heat treated in air at $T = 1200^\circ\text{C}$ and (b) cleavage of the silica gel-glass doped with them. It is seen that these nanoparticles are the grains ~ 50 nm in diameter, and the maximum size of their agglomerates is ~ 300 nm. Similar grains and agglomerates are also clearly discernible in the doped

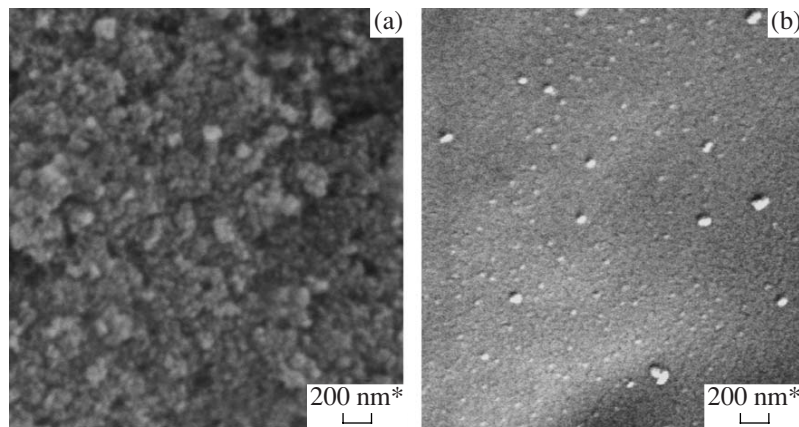


Fig. 1. Electron microphotographs of (a) Cr-containing nanoparticles and (b) silica gel-glass doped with them.

glass, and it is clear that their mean size is smaller than that of the nanoparticles introduced.

Curve *1* in Fig. 2 is the LAS of the silica gel-glass doped with the Cr-containing nanoparticles, where the arrows point to the positions of the weak spectral band peaks. For comparison, curve 2 in this figure is the LAS of the undoped silica glass that is synthesized under the same temperature and time conditions. It is seen that the doped glass in the visible and near-IR spectral regions is characterized by higher light scattering, weak broad absorption bands with $\lambda_{\max} \approx 400$ and 560 nm, and a monotonic decrease in the optical density in the range 700–1000 nm. In the UV spectral region, this glass is characterized by an intense band with $\lambda_{\max} = 225$ nm (the peak value is determined after the preliminary subtraction of curve 2 from curve *1*) and a slightly discernible “shoulder” at $\lambda \approx 310$ nm.

Figure 3 presents the LSs of the (curve *1*) Cr-containing nanoparticles and (curves 2–4) silica gel-glass doped with them recorded with the halfwidths of band

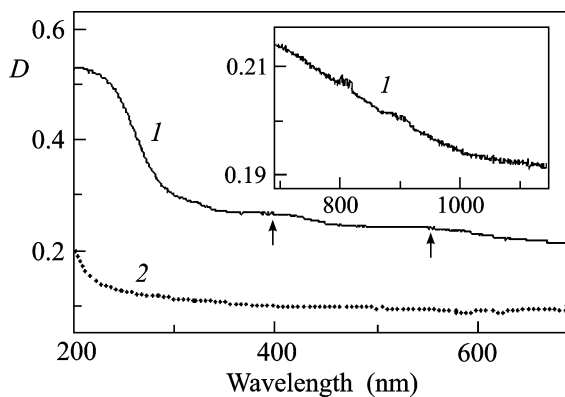


Fig. 2. Light attenuation spectra of (*1*) silica gel-glasses doped with Cr-containing nanoparticles and (*2*) undoped glass. The sample thickness is 3 mm.

excitation ($\Delta\lambda_{\text{exc}}$) and recording ($\Delta\lambda_{\text{rec}}$) equal to 2 nm at different excitation wavelengths (λ_{exc}). The inset presents the LSs of both samples compared in the region of the Cr^{3+} *R*-lines recorded at $\Delta\lambda_{\text{rec}} = 0.1$ nm. It is seen that the LS of the nanoparticles at $\lambda_{\text{exc}} = 550$ nm corresponds to the Cr^{3+} ions in the trigonally distorted strong octahedral crystal field [8]. No luminescence bands attributed to other optical Cr centers have been revealed for these nanoparticles at different λ_{exc} values. Under excitation in the visible spectral region, the incorpora-

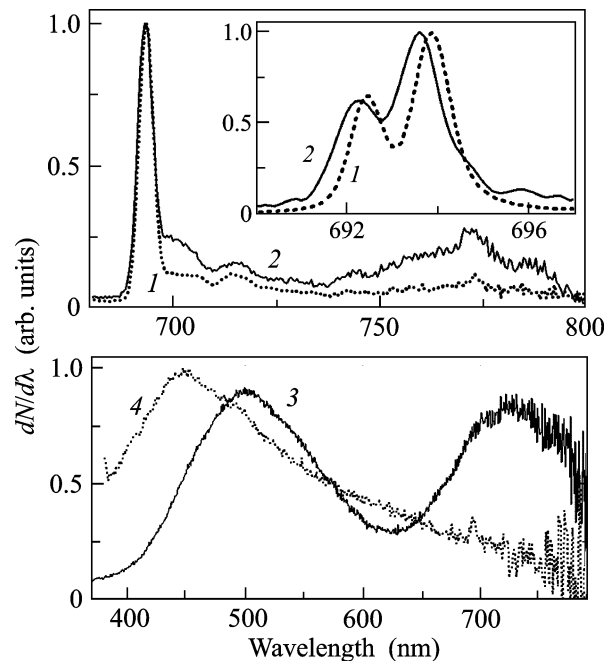


Fig. 3. Luminescence spectra of (*1*) Cr-containing nanoparticles and (*2–4*) silica gel-glass doped with them at $\lambda_{\text{exc}} =$ (*1*, *2*) 550, (*3*) 280, and (*4*) 350 nm; $\Delta\lambda_{\text{rec}} =$ (in the inset) 0.10 and (general spectra) 2 nm.

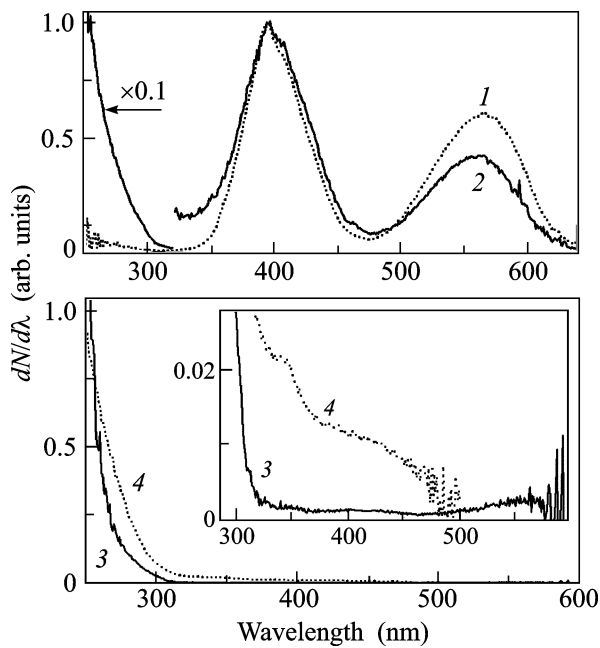


Fig. 4. Luminescence excitation spectra of (1) Cr-containing nanoparticles and (2–4) silica gel-glass doped with them at $\lambda_{\text{rec}} =$ (1, 2) 694, (3) 730, and (4) 520 nm.

tion of the Cr-containing nanoparticles into the glass is accompanied by a short-wavelength shift of the R -line barycenters by about 0.3 nm ($\approx 6.2 \text{ cm}^{-1}$) and their broadening (cf. curves 2 and 1 in the inset), as well as by an increase in the luminescence intensity of the poor structure bands in the range 700–800 nm. Under the excitation of this glass in the UV spectral region ($\lambda_{\text{exc}} = 280 \text{ nm}$), instead of the narrow bands, there appear two broad luminescence bands with $\lambda_{\text{max}} \approx 500 \text{ nm}$ and 730 nm (curve 3), while at $\lambda_{\text{exc}} \approx 350 \text{ nm}$, the broad band with $\lambda_{\text{max}} = 450 \text{ nm}$ (curve 4). The glass excitation in the near-IR region ($\lambda_{\text{exc}} = 800 \text{ nm}$) is not accompanied by luminescence.

Figure 4 presents the LESs of the (curve 1) Cr-containing nanoparticles and (curves 2–4) gel-glass doped with them at different recording wavelengths λ_{rec} . It is seen that at $\lambda_{\text{rec}} = 694 \text{ nm}$, the LES of nanoparticles includes two intense broad bands, which are typical of Cr^{3+} ions in the strong octahedral crystal field, with $\lambda_{\text{max}} \approx$ (a higher-intensity band) 395 and 560 nm, and a low-intensity band at $\lambda \approx 260 \text{ nm}$. A similar spectrum in the visible region is also retained for the silica glass doped with these particles, while an intense broad band appears in the UV region with the maximum at $\lambda < 250 \text{ nm}$ (curve 2). The LESs at $\lambda_{\text{rec}} =$ (curve 3) 730 and (curve 4) 520 nm also exhibit an intense UV band with significantly different shapes of the long-wavelength “wings” for the mentioned λ_{rec} values.

A relatively small decrease in the main size of the grains and agglomerates of the Cr-containing nanoparticles introduced in the sol under glass sintering (cf.

Figs. 1a and 1b) allows us to conclude that sol–gel synthesis with no melt stage makes it possible to radically weaken the aggressive effect of the matrix on the nanoparticles introduced. According to the LASs (see Fig. 2), the incorporation of the nanoparticles into the glass leads not only to the appearance of the spin-allowed absorption bands ${}^4A_2 \rightarrow {}^4T_1$ ($\lambda_{\text{max}} \approx 400 \text{ nm}$) and ${}^4A_2 \rightarrow {}^4T_2$ ($\lambda_{\text{max}} \approx 560 \text{ nm}$) of Cr^{3+} ions typical of these nanoparticles [2], but also to the appearance of new bands that are not associated with these nanoparticles in the UV, visible, and near-IR spectral regions. Naturally, under this incorporation, light scattering increases slightly, but noticeably.

According to the Tanabe–Sugano diagram, a considerable short-wavelength shift of the luminescence R lines of the Cr-containing nanoparticles in their incorporation into the glass (cf. curves 1 and 2 in the inset in Fig. 3) points to an increase in the local crystal field force, while the broadening of these bands, to an increase in the range of variation of this force. It is reasonable to expect this situation as the distances between the Cr atoms and ligand decrease, and we think that it is most probably caused by the isotropic compression of the Cr-containing nanoparticles by the glass matrix; the degree of this compression depends on their size. A marked increase in the luminescence intensity of the poor structure bands on the side of the longer wavelengths from the R lines is probably caused, to a great extent, by an increase in the electron–phonon coupling. The appearance of new broad bands in the visible region of the LS of the glass (see Fig. 3, curves 3 and 4) could reasonably be attributed to the formation of the optical Cr centers by the ions present in the dissolved part of the Cr-containing nanoparticles. In particular, the band with $\lambda_{\text{max}} \approx 730 \text{ nm}$ can certainly be assigned to the isolated Cr^{3+} ions in a weak octahedral local field typical of the glass [9].

The existence of the isolated Cr^{3+} ions in the nanoparticles in the glass is also confirmed by the analysis of the LESs (see Fig. 4). First, this is indicated by the similarity of the LESs in the visible region at $\lambda_{\text{rec}} = 694 \text{ nm}$ for the Cr-containing nanoparticles and the glass doped with them (cf. curves 1 and 2), pointing to the conservation of the structure of these nanoparticles. Second, the presence of pronounced traces of bands ${}^4A_2 \rightarrow {}^4T_2$ and ${}^4A_2 \rightarrow {}^4T_1$ in the LES of the glass at $\lambda_{\text{rec}} = 730 \text{ nm}$ (see curve 3 in the inset) indicates that the corresponding luminescence band is attributed to the isolated Cr^{3+} ions distributed in the glass. A lower relative intensity of the band ${}^4A_2 \rightarrow {}^4T_1$ in this spectrum, as compared to that of the LES of the Cr^{3+} ions in the nanoparticles, might point to an increase in the probability of the quenching of the 4T_1 state when these ions transfer from the nanoparticles to the glass. A marked short-wavelength shift of the barycenter of the band ${}^4A_2 \rightarrow {}^4T_2$ in the LES of the glass (cf. curves 1 and 2) confirms the conclusion that the nanoparticles are com-

pressed by the silica matrix.¹ Considerably more efficient luminescence excitation of the Cr³⁺ centers of both types in the UV spectral region can be explained by the excitation transfer from the structural defects of the matrix [10] and/or from the Cr optical centers in the other charged state. In this case, in view of the absence of the excitation transfer from the isolated optical Ln³⁺ centers to the CeO₂:Ln³⁺ nanoparticles in the silica gell-glasses [11], it is reasonable to suppose that this transfer for the Cr-containing nanoparticles takes place only from the centers located at the nanocrystal–glass interface.

We note that, due to the oxidation conditions of the synthesis, the Cr atoms at higher oxidation degrees appear in the glass along with Cr³⁺. In this case, the substitution of the isovalent Cr atoms for the Si atoms in the [SiO₄]⁴⁻ polyhedra is quite probable, because it does not require local charge compensation. However, according to the geometrical criterion [12], a large ion radius of the four-coordination ion Cr⁴⁺, $r \approx 0.55$ Å against $r \approx 0.40$ Å for Si⁴⁺ [12] is not optimal for this substitution, and we can suggest that [CrO₆]⁸⁻ polyhedra exist along with [CrO₄]⁴⁻ polyhedra. A more favorable situation for the substitution of the Si atoms in the [SiO₄]⁴⁻ polyhedra in accordance with the above criterion takes place for the four-coordination Cr⁵⁺ ions ($r \approx 0.49$ Å) and Cr⁶⁺ ions ($r \approx 0.40$ Å) [12]. The necessary local charge compensation can be provided, for example, by silicon vacancies: one such vacancy compensates the excessive charges of either two Cr⁶⁺ ions or four Cr⁵⁺ ions.

As experimental evidence of the formation of the optical Cr⁴⁺ centers in the glass, we point to the presence of the absorption band in the range $600 \leq \lambda \leq 1000$ nm (see Fig. 2) corresponding to the transitions ${}^3A_2 \rightarrow {}^3T_1$, 3T_2 of these ions in the tetrahedral environment [13]. We believe that the main cause of the absence of their luminescence (it is characterized by the broad band at $\lambda \sim 1.2$ μm [7]) is its quenching by spending the excitation energy on the vibrations of hydroxyl ions whose concentration is about 0.3 wt %, as determined by the known spectroscopy method [14].

One piece of evidence of the formation of the [CrO₄]²⁻ polyhedra is the presence of the intense absorption band with $\lambda_{\max} \approx 225$ nm in the LASs (see Fig. 2). It is known [15] that these centers are characterized by absorption in two bands of charge transport $O^{2-} \rightarrow Cr^{3+}$ with $\lambda_{\max} \approx 230$ and 360 nm. Probably, the luminescence band with $\lambda_{\max} \approx 500$ nm is attributed to the [CrO₄]²⁻ polyhedra (see Fig. 3, curve 3). The LES of this band includes the corresponding excitation

bands (see Fig. 4, curve 4). Since the Cr⁶⁺ ions with an empty 3*d* shell have no optical transitions in the spectral region under consideration, this luminescent band can be attributed to luminescence from the excited state of charge transport. This interpretation is supported by the position of the luminescence band of the stable Cr⁵⁺ centers in the silica glass at a much longer wavelength $\lambda_{\max} \approx 610$ nm at $\lambda_{\text{exc}} \approx 364$ nm [6]. The appearance of the low-intensity “shoulder” in the LS of the glass at $\lambda \approx 600$ nm and $\lambda_{\text{exc}} = 350$ nm (see Fig. 3, curve 4) indicates that the stable Cr⁵⁺ centers at low concentration are formed in our case. Obviously, they are also responsible for a broad low-intensity excitation band at $\lambda \sim 450$ nm in the LES of the glass with $\lambda_{\text{rec}} = 520$ nm (see Fig. 4, curve 4), which coincides with the absorption transition ${}^2T_2 \rightarrow {}^2E$ of the six-coordination Cr⁵⁺ ions [16]. The broad luminescence band with $\lambda_{\max} \approx 450$ nm (see Fig. 3, curve 4) is probably related to the presence of molecular silicon oxide in the glass [10].

To conclude, we have shown the possibility of conserving the spectral luminescent properties and, accordingly, the structure of the heat-resistant Cr-containing nanoparticles introduced at the sol stage in the direct sol–gel-glass transition. The absence of the melt stage radically weakens the dissolution of these nanoparticles at the xerogel vitrification stage, and the matrix effect manifests itself in their isotropic compression, in a considerable increase in the spread of the local field force acting on the Cr³⁺ ions, and in an increase in the intensity of the electron vibration bands in the luminescence spectrum. The Cr ions in the dissolved nanoparticles form the octahedral Cr³⁺ centers with a “weak” ligand field, as well as the optical centers of the high-charge Cr (Cr⁶⁺, Cr⁵⁺, and Cr⁴⁺).

This work was supported in part by the Belarusian Republican Foundation for Fundamental Research (project no. F08R-128).

REFERENCES

1. V. N. Sigaev, S. S. Soukhov, P. D. Sarkisov, et al., *Phys. Chem. Glasses* **46**, 236 (2005).
2. G. E. Malashkevich, V. A. Lapina, and P. P. Per-shukevich, *Izv. Ross. Akad. Nauk, Ser. Fiz.* **70**, 1659 (2006).
3. P. J. Deren, E. Lukowiak, M. Suszynska, et al., *Zh. Prikl. Spektrosk.* **62** (4), 53 (1995).
4. W. Strek, E. Lukowiak, P. J. Deren, et al., *SPIE Proc.* **3176**, 249 (1997).
5. W. Strek, P. J. Deren, E. Lukowiak, et al., *J. Non-Cryst. Solids* **288**, 56 (2001).
6. V. I. Glazkov, K. M. Golant, Yu. S. Zavorotnyi, et al., *Fiz. Khim. Stekla* **28**, 286 (2002).
7. V. V. Dvoirin, E. M. Dianov, V. M. Mashinsky, et al., *Quant. Electron.* **31**, 996 (2001).

¹ Causes of the appearance of a pronounced small peak at $\lambda = 594$ nm under this compression, which can be assigned to the spin-forbidden transition ${}^4A_2 \rightarrow {}^2T_1$, will be considered elsewhere.

8. S. V. Grum-Grzhimailo, L. B. Pasternak, and R. K. Sviridov, in *Crystal Spectroscopy, Proc. of the Symp. on Spectroscopy of Crystals with Rare-Earth Elements and Elements of Iron Group*, Ed. by S. V. Grum-Grzhimailo and P. P. Feofilov (Nauka, Moscow, 1966), p. 195 [in Russian].
9. I. B. Artsybysheva, S. G. Lunter, N. T. Timofeev, and Yu. K. Fedorov, *Fiz. Khim.* **16**, 625 (1990).
10. A. R. Silin and A. N. Trukhin, *Point Defects and Elementary Excitations in Crystalline and Glassy SiO₂* (Zinatne, Riga, 1982) [in Russian].
11. G. E. Malashkevich, G. I. Semkova, A. P. Stupak, and A. V. Sukhodolov, *Fiz. Tverd. Tela* **46**, 1386 (2004) [*Phys. Solid State* **46**, 1425 (2004)].
12. B. K. Vainshtein, V. M. Fridkin, and V. L. Indenbom, *Modern Crystallography* (Nauka, Moscow, 1982; Springer, Berlin, 1982), Vol. 2.
13. C. Anino, J. Thery, and D. Vivien, *Optics Mater.* **8**, 121 (1997).
14. V. K. Leko and O. V. Mazurin, *Properties of Quartz Glass* (Nauka, Leningrad, 1985) [in Russian].
15. Cz. Koepke, K. Wisniewski, M. Grinberg, et al., *J. Phys.: Condens. Matter* **13**, 2701 (2001).
16. M. Herren, H. Nishiuchi, and M. Morita, *J. Chem. Phys.* **101**, 4461 (1994).

Translated by E. Perova